Describing Phenotypic Subtypes of GBM in DWI Imaging in Relation to its Genotypic Subtypes

by

Mohammed Ahmed Hasen

A Thesis submitted to the Faculty of Graduate Studies of

The University of Manitoba

in partial fulfilment of the requirements of the degree of

MASTER OF SCIENCE

Department of Surgery
University of Manitoba
Winnipeg

Table of Contents

Abstract

Glioblastoma (GBM) is the most lethal primary brain tumour of the central nervous system, and has an unpredictable response to treatment with wide range of survival. There have been many attempts to identify factors that influence survival. We investigated the possible association between diffusion MRI, molecular signature, and survival of patients with GBM. This is a retrospective study conducted in Winnipeg (Health Sciences Center) for patients with GBMs from January 2015 to January 2018. In 93 patients, correlating normalized apparent diffusion coefficient (nADC) to time to death in days showed a Spearman's rho correlation value of 0.244, indicating a weakly positive linear correlation. IDH mutation status in relation to nADC was found to be significant (mean difference of 0.38 and p-value of 0.015). The log-rank (Mantel–Cox) of nADC with cut-off point of 1.1725 was found to be significant (p-value of 0.046). The median survival was 11.5 months for nADC>1.1725 .vs 7.5 months for nADC<1.1725. The Cox regression multivariate analysis that included nADC (cut-off pint of 1.1725), age, nADC, IDH-mutation status, and extent of resection showed that age (p-value of 0.016) and nADC (p-value of 0.039) are statistically significant. Individuals with nADC <1.1725 were associated with an increased mortality hazard of 69% compared to individuals with nADC >1.1725 after adjusting for covariates of age, gender, and IDH mutation status. Individuals <70-year-old had a reduced mortality hazard of 47% compared to individuals >70-year-old old after adjusting for covariates of nADC, IDH mutation status, and extent of resection. In conclusion, nADC might have some value in identifying GBM patients with worse survival via IDH-mutation status.

Statement

I hereby confirm that the material presented in this project is the result of my own effort and any material from other sources/authors have been acknowledged in text and listed in the reference section.

Abbreviations

ADC	Apparent diffusion coefficient
AUC	Area under the curve.
CNS	Central nervous system
DTI	Diffusion tensor imaging
DWI	Diffusion-weighted imaging
FLAIR	Fluid attenuation inversion recovery
GBM	Glioblastomas
IDH	Isocitrate dehydrogenase
KPS	Karnofsky performance status
LOH 1p/19q	Loss of heterozygosity of 1p/19q
MGMT	O6-methyl guanine-DNA-methyltransferase
MRI	Magnetic resonance imaging.
nADC	Normalized apparent diffusion coefficient
NAWM	Normal-appearing white matter
OS	Overall survival.
PACS	Picture Archiving and Communication System
PET	Positron emission tomography
PFS	Progression-free survival
PWI	Perfusion weighted imaging
RANO	Response assessment in neurooncology
ROC	Receiver operating characteristic
T1WI	T_1-weighted imaging
T2WI	T_2-weighted imaging
WHO	World health organization

1. Introduction

- 1.1 Introduction to GBM
- 1.2 The Issue of Survival of GBM
- 1.3 The Need for Better Survival Markers of GBM
- 1.4 The Search for Noninvasive Survival Markers for GBM; Role of MRI
- 1.5 Diffusion MRI as a Noninvasive Survival Marker for GBM
- 1.6 Our Hypothesis

1.1 Introduction to GBM

Astrocytomas are the most common primary brain tumours (Kleihues & Cavenee, 2000). According to the classification system of the World Health Organization (WHO), grade IV astrocytomas are known as glioblastoma (GBM) and are the most lethal primary brain tumour in the adult population (Louis et al., 2016).

The origins of the modern classification systems of CNS tumors can be traced back to Bailey and Cushing in 1926 that was based on microscopic histopathological feature (Bailey & Cushing, 1926). Following that, a number of other tumor classification systems were proposed, but didn't replace Bailey and Cushing classification system. In 1979, the WHO published their first edition of classification system of CNS tumors that became the current accepted standard (Zulch, 1979). In the updated 2016 WHO classification system of CNS tumors, an integration of a microscopic features and molecular/genetic factors can be found in defining tumors subtypes (Louis et al., 2016).

Before the 2016 WHO edition, the vast majority of infiltrating gliomas fell into one of three categories: astrocytomas, oligoastrocytomas, and oligodendrogliomas. The distinction was based mostly on the morphological assessment. This classification brought some insight about tumor behavior and survival, but there was still unexplained variability. Recently, it was recognized that IDH mutation status might explain some of this variability. In GBM, Parsons and colleagues found that the OS in IDH1-mutant GBM was more than 3-fold the survival of IDH1 wild-type GBM (Parsons et al., 2008). This finding was replicated by many studies following that which indicates that IDH1 mutation status is a favorable prognostic factor in adult gliomas (Brat et al., 2020).

1.2 The Issue of Survival with GBMs

The clinical presentation of a patient with a newly diagnosed GBM can be highly variable and dependant on the site and size of the lesion (Davis, 2016). The current standard treatment for a patient with a newly diagnosed GBM is composed of maximal safe surgical debulking, followed by concurrent radiation treatment and chemotherapy (Stupp et al., 2005). Therefore, GBM treatment requires a multidisciplinary approach that involves many medical services, including neurosurgery, medical oncology, and radiation oncology.

Generally, the overall prognosis of high-grade astrocytomas (especially GBMs) is poor, although many treatment modalities have evolved throughout the years (Salcman, 2001). The average survival time from diagnosis to death ranges from 12 to 18 months. With the standard treatment applied, more than 70% of GBMs invariably progress and, unfortunately, might require a second treatment (Mallick, Benson, Hakim, & Rath, 2016).

1.3 The Need for Better Survival Markers for GBMs

The highly variable response to treatment of GBM establishes the need for well-validated survival biomarkers that might be able to predict response to treatment, survival, and progression (Herbert et al., 2011). This can be helpful to support the therapeutic decision-making process when combined with other factors linked to survival and treatment response like age, molecular profile, and extent of resection (Saksena et al., 2010). Such guidelines could guide patient care and avoid side effects from ineffective therapies.

There have been many efforts to search for survival-related factors in the literature that could have predictive value for patient outcomes (Saksena et al., 2010). These markers

can be classified as clinical, radiological, histopathological/genetic, and therapeutic factors. Regarding clinical markers, several parameters have been linked to the survival and of GBMs. The list mainly includes age at the time of diagnosis and the patient's Karnofsky Performance Status (KPS). Multiple studies have examined the possible clinical association of age and KPS in GBMs. The evidence suggests that advanced age and low KPS are independently associated with the poor survival rates of patients with GBMs (Neal et al., 2013)

Regarding radiological factors, specific tumour characteristics on imaging have been linked to survival. The basic radiological elements are the volume and location of the tumour. Along with these structural features described by imaging and linked to survival, several specific imaging modalities have been linked to survival and treatment. Most of these imaging modalities are related to magnetic resonance imaging (MRI).

Certain histopathological and genetic markers, including isocitrate dehydrogenase-1 (IDH-1) mutation status, O6-methyl guanine-DNA-methyltransferase (MGMT) promoter methylation status, 1p/19q codeletion status, and Ki67 have been studied as potential prognostic markers of survival with variable degrees of sensitivity and specificity. IDH mutation status and MGMT promoter methylation status are independently associated with favourable outcomes in GBM patients. It is becoming increasingly evident that the more exact the histopathologic/genetic evaluation of the tumour, the more effective the treatment planning (Çoban et al., 2015). Regarding therapeutic markers studied in GBMs, the extent of resection, radiation therapy, and chemotherapy are all linked to survival with GBMs (Rossignol, Srinageshwar, & Dunbar, 2020). Many clinical trials are still in progress to validate the specifics of treatment modalities such as dose, fractionation, and timing.

1.4 The Search for Noninvasive Survival Markers for GBM: Role of MRI

Currently, the comprehensive assessment of patients with newly diagnosed GBMs requires tissue samples from the tumour. This can be done invasively through biopsy or surgical debulking. However, a noninvasive assessment of GBM prognosis would be particularly welcome for treatment planning of GBM patients in the era of personalized medicine.

The standard imaging modality for detecting and assessing tumours in patients with GBMs depends heavily on conventional MRI (Macdonald, Cascino, Schold Jr, & Cairncross, 1990). The standard conventional MRI employed for the investigation of patients with newly diagnosed GBMs includes T1-weighted imaging (T1WI), T2-weighted imaging (T2WI), fluid attenuation inversion recovery (FLAIR), T2*WI gradient echo sequence, and contrast-enhanced T1WI. Contrast-enhancing imaging can guide resection planning and estimate prognosis in the context of GBMs (Çoban et al., 2015); however, although most of the conventional MRI sequences can provide information on GBMs' gross structural features, they cannot provide functional information that might be more relevant to treatment response and prognosis.

This lack of functional information makes the need for novel imaging biomarkers essential and explains the growing interest in that field (Aum et al., 2014; Friedmann-Morvinski, 2014). Novel imaging biomarkers would aid in selecting patients who would most likely benefit from aggressive treatment of maximal surgical resection and adjuvant treatment. The biomarkers would then also help prioritize these patients' access to treatment, which could eventually have a positive impact on their OS and PFS (Madsen, Hellwinkel, & Graner, 2015). Many advanced imaging modalities have been studied as possible attractive

options in comparison to to more invasive approaches. Positron emission tomography (PET) uses injected radiotracers to target specific metabolic and molecular markers. Perfusion weighted imaging (PWI) provides a measure of tumour perfusion. Last, diffusion MRI techniques have been investigated for use in GBM management (Drake-Pérez, Boto, Fitsiori, Lovblad, & Vargas, 2018; Shukla et al., 2017; van Dijken et al., 2019).

MRI allows for the noninvasive characterization of brain tumours and plays a major role in the diagnosis and management of patients with GBM for two major reasons. First, it has the capacity for the detection of soft-tissue contrast necessary to provide superior anatomical structural information. Second, different MR sequences and modalities can reflect key components of the physiology of tumours, including blood flow, hypercellularity, and metabolic microenvironment.

Magnetic resonance spectroscopy (MRS) provides details about the metabolic composition of tissues. The high Choline to Creatinine ratio (Cho/Cr ratio) is thought to be a malignant feature and was found to be useful in distinguishing histological grade of gliomas (Pope, Prins, et al., 2012). Also, there is emerging data to suggest a correlation between Cho/Cr ratio and IDH-mutation status indicating that it might be a potential noninvasive biomarker for evaluation of the IDH status gliomas (Bulakbasi, Kocaoglu, Örs, Tayfun, & Ügöz, 2003). In addition to MRS, IDH mutation status was found to be associated with with hypoxia and multiple related metabolites including hypoxia-induced factor-1α. Based on that, perfusion MRI was suggested to predict IDH-mutation status indirectly. The IDH1-mutant glioma was found to have a decreased relative cerebral blood volume (rCBV) compared with the IDH1-wild glioma regardless of histologic grade (Deike et al., 2016).

1.5 Diffusion MRI as a Noninvasive Survival Marker for GBMs

Diffusion-weighted magnetic resonance imaging (DWI) is a special MRI sequence that uses data related to the diffusion of water molecules to generate contrast in images (Louis et al., 2016; Ohgaki & Kleihues, 2013; Seystahl et al., 2020). Diffusion MRI is based on the Brownian motion of water molecules, and the field is evolving with the advancement of technology (Bulakbasi et al., 2004). More advanced techniques of diffusion MRI have been introduced, but few have been studied in the context of GBM (Drake-Pérez et al., 2018). Advanced diffusion MRI techniques include intravoxel incoherent motion, diffusion kurtosis imaging, restriction spectrum imaging, and stretched exponential (Chakhoyan et al., 2018; Khan et al., 2018; Krishnan et al., 2017).

The diffusion imaging sequence allows the noninvasive mapping of the diffusion process in biological tissues. This can reveal details about tissue architecture in normal or pathologic states. DWI holds considerable promise for improving the diagnosis of GBM patients in the first presentation and recurrent status. Moreover, research has shown that DWI plays an important role in predicting the grade of tumours and linking that information to treatment response and survival (Schmainda, 2012; Yan et al., 2017).

Restricted diffusion can also be seen in areas of high cellularity (Chenevert, Sundgren, & Ross, 2006; Gauvain et al., 2001). This can be explained by the fact that increasing cellularity reduces the interstitial space of water molecules, leading to restricted diffusion. Based on that principle, ADC has been linked to the body's response to chemotherapy (Chen et al., 2005; Tomura et al., 2006) and used to predict prognosis in the treatment of GBMs (Babsky, Hekmatyar, Zhang, Solomon, & Bansal, 2006; Pope, Qiao, et

al., 2012). Previous work has shown that restricted diffusion could be correlated with the area of contrast enhancement in MRI (Gupta et al., 2011). The use of ADC to assess the response to surgery in these patients has been recently investigated (Shankar et al., 2016).

1.6 Our Hypothesis

There is an enormous need to find personalized and targeted treatment options for patients with GBM (Nuzzo et al., 2020; Zhang & Liu, 2020), We investigated the possible association between diffusion MRI metrics and survival outcome. We further investigated the possible relationship between molecular signature of GBMs and diffusion MRI metrics.

2. Methods

- 2.1 Patient selection.
- 2.2 Image acquisition.
- 2.3 Image analysis.
- 2.4 Therapeutic data.
- 2.5 Molecular analysis.
- 2.6 Pathological data.
- 2.7 Ethics considerations.
- 2.8 Statistical analysis.

2.1 Patient Selection

This retrospective study was conducted at the Health Sciences Center in Winnipeg. From January 2015 to January 2018, all patients with histologically confirmed GBM were identified from the medical and pathological record database. Diagnosis was made based on pathological tissue examination after biopsy or surgical resection of a tumour. Of patients meeting final inclusion, a minimum of two years of follow-up was available. All identified **patients were screened further using the following inclusion criteria:**

- Adult population (age >18)
- Supratentorial tumor location
- Availability of high-quality preoperative MR imaging, including ADC/DWI maps
- Availability of molecular subgroup analysis
- Availability of basic clinicopathologic information
- Availability of survival information

The list of pre-operative conventional MRI sequences required included pregadolinium T1-weighted images, postgadolinium T1-weighted images, T2-weighted images, and axial FLAIR images. The list of required components of diffusion MRI sequences included DWI and ADC maps.

Molecular and genetic data were obtained from pathology records. Using the current WHO classification system published in 2016, at least two experienced neuropathologists performed the histopathological diagnosis and grade assessment for each patient's tumour. The list of molecular and genetic information reported includes IDH-1 mutation status,

ATRX immunoreactivity, Ki67 index, and MGMT. Clinical details and survival were obtained from the institutional medical record. Patient with intratumoural hemorrhage that precluded calculation of nADC were excluded.

2.2 Image Acquisition

All patients ultimately included in the study underwent preoperative MRI before medical or surgical intervention. A standard brain tumour imaging protocol that included Sagittal T1 images (fast spin-echo images using single-shot, echo-planar imaging with 500 ms repetition time (TR), 22.8 ms echo time (TE), 220 mm field of view (FOV), 320 x 192 matrix size, 5 mm section thickness, and a 1.5 mm intersection gap), Axial T2 (fast spin-echo images using 8000 ms TR, 120 ms TE, 220 mm FOV, 256 x 254 matrix size, 5 mm section thickness, and a 1.5 mm intersection gap), FLAIR (fast spin-echo images using 8000 ms TR, 120 ms TE, 2000 ms TI, 220 mm FOV, 256 x 254 matrix size, 5 mm section thickness, and a 1.5 mm intersection gap) and DWI/ADC images (single-shot echo-planar imaging with 8000 ms repetition time TR, 73.6 ms TE, 260 mm FOV, 160 x 192 matrix size, 5 mm section thickness, a 1.5 mm intersection gap, and 1000 and 0 b-values in three orthogonal directions) and post gadolinium axial and coronal T1 weighted (fast spin-echo images using single-shot, echo-planar imaging with 500 ms repetition time (TR), 22.8 ms echo time (TE), 220 mm field of view (FOV), 320 x 192 matrix size, 5 mm section thickness, and a 1.5 mm intersection gap) images.

Other MRI sequences included, pre- and post-contrast T1-weighted images were acquired as fast spin-echo images using single-shot, echo-planar imaging with 500 ms repetition time (TR), 22.8 ms echo time (TE), 220 mm field of view (FOV), 320 x 192 matrix

size, 5 mm section thickness, and a 1.5 mm intersection gap. T2 images were acquired as fast spin-echo images using 8000 ms TR, 120 ms TE, 220 mm FOV, 256 x 254 matrix size, 5 mm section thickness, and a 1.5 mm intersection gap. FLAIR images were acquired as fast spin-echo images using 8000 ms TR, 120 ms TE, 2000 ms TI, 220 mm FOV, 256 x 254 matrix size, 5 mm section thickness, and a 1.5 mm intersection gap. Diffusion MRI sequences (DWI and ADC maps), were acquired using single-shot echo-planar imaging with 8000 ms repetition time TR, 73.6 ms TE, 260 mm FOV, 160 x 192 matrix size, 5 mm section thickness, a 1.5 mm intersection gap, and 1000 and 0 b-values obtained in three orthogonal directions.

2.3 Image Analysis

MR imaging analysis was performed on a picture archiving and communication system (PACS) workstation under the supervision of a fellowship-trained neuroradiologist. True restricted diffusion was defined as area that had both hyperintensity on the DWI map and hypointensity on the ADC map (Drake-Pérez et al., 2018). The following process was used to quantify the amount of restriction diffusion within each tumour's area. First the PACS images were analyzed to identify all areas of intratumoral true restricted diffusion defined by both ADC and DWI. We identified areas of true restricted diffusion when the area chosed hyperintense on DWI sequence and hypointense on the ADC sequence. The degree of restriction was quantified by the lowest average ADC value within each area of restricted diffusion identified.

Each area was then thoroughly analyzed using the PACS software to identify the area with lowest ADC measurement among all areas screened. The PACS software (Impax-Agfa

Care) offers a freedom markup tool that determines the average quantitative ADC value for the area chosen in axial view (Diagram 1).

To counteract differences in image acquisition between patient, the data was normalized by comparing the lowest ADC value to normal appearing white matter (NAWM) on the contralateral side. This created a normalized ADC value (nADC) derived from there following calculation: minimal ADC/NAWM. Thus, a lower nADC value is indicative of a tumour with a higher degree of restricted diffusion. An example

In cases where intratumoural hemmorahge was present, the calculation of minimum ADC was unreliable and these patients were not included. The observer was blinded to the clinical data at during the period of MRI data acquisition.

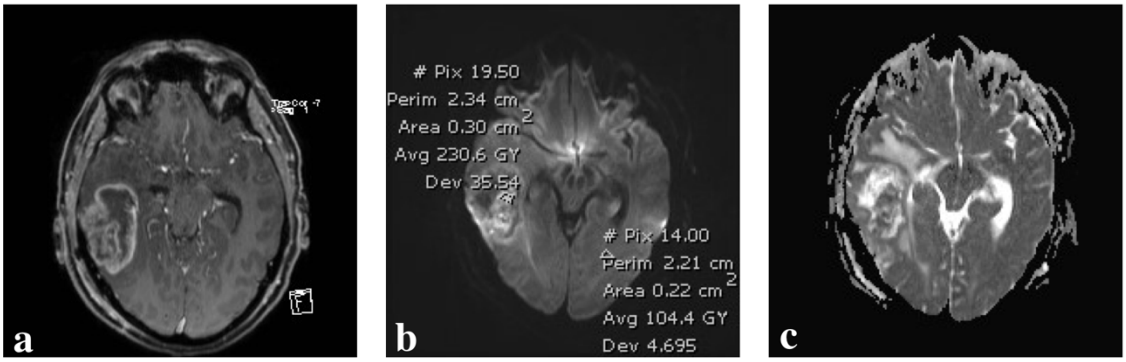

Diagram 1 (a) T_1 weighted image with contrast. (b) ADC map. (c) DWI map. The picture in (b) shows the freedom markup tool offered by the PACS software (Impax-Agfa Care) to measure the average quantitative ADC value for the area chosen in axial view (value of 230.6). The contralateral NAWM is then measures using the same tool (value of 104.4). nADC becomes then 2.2 in this example. ADC- Apparent Diffusion Coefficient; DWI- Diffusion Weighted Images. nADC Normalized Apparent Diffusion Coefficient; NAWM Normal-appearing white matter .

2.4 Therapeutic Data

Surgical treatment data were collected for each patient from imaging records and classified into biopsy, partial resection, or total/near-total resection based on the immediate postoperative imaging, which was available for all patients based on the radiology report.

2.5 Molecular Analysis

Molecular analysis variables were collected from each patient in our study that includes IDH, ATRX, BRAF V600E, H3F3A, H3F3B, HIST1H3B , and TERT promoter mutational status, 1p/19q codeletion status as well as MGMT methylation status. Molecular and genetic data were obtained from pathology records. The molecular analysis (immunohistochemistry [IHC], using Fluorescence In Situ Hybridization [FISH], PCR and gene sequencing) was performed on formalin-fixed paraffin-embedded tissue obtained at the time of surgical diagnosis. Satisfactory pathological examination was ensured for each patient; otherwise, the patient was excluded from the study. Using the current WHO classification system published in 2016, at least two experienced neuropathologists performed histopathological diagnosis and grade assessment for each patient's tumour.

IDH mutation status was determined first by immunohistochemical analysis using a mutation-specific monoclonal antibody against IDH1 R132H (clone: HO9, dianova, Hamburg, Germany). IDH1 and IDH2 gene sequencing were performed only on IDH1 R132 negative glioblastoma in patients younger than 55 years of age as patients of 55 years of age or older are considered IDH-wildtype if IDH1 R132H IHC was negative. Mutation in IDH1, IDH2, H3F3A, H3F3B, HIST1H3B, and TERT promoter genes were determined by Agena MassARRAY system that couples mass spectroscopy with end-point PCR. ATRX mutational

status was determined by immunohistochemical analysis using anti-ATRX antibody (Sigma life science, rabbit polyclonal). MGMT promoter methylation were performed in all glioblastoma by MSRE-qPCR (Methylation Sensitive Restriction Enzyme digestion followed by real time TaqmanPCR analysis) method using Zymo Research OneStep qMethyl – Life reagents and custom MGMT promoter specific primers/probes. Sample is considered to be methylated if the methylation score is greater than 9%. Loss of heterozygosity (LOH 1p/19q) was examined using FISH studies). All immunohistochemistry analysis were done in the Health Sciences Center-Winnipeg. The 1p19q codeletion test was done in PhenoPath Laboratories, Seattle, Washington, while the MGMT methylation analysis and Agena MassArray was done in Calgary Laboratory Services.

2.6 Outcome Measures

Our study's primary outcome of interest is OS which was defined as the interval between the date of tissue acquisition and the date of death for patients who died within the study follow-up period or the last of follow-up for patients who did not. 86 patients in our study reached the primary endpoint of the study (i.e., death) during the follow-up period constituting 92.5% of all patients included in the study

2.7 Ethics Considerations

The Research Ethics Board of the University of Manitoba authorized this study. The study protocol was in accordance with institutional review board guidelines.

2.8 Statistical Analysis

Independent variables were first evaluated as bivariate correlations after which statistically significantly variables were included in the multivariate analysis. Associations were further analyzed using Kaplan–Meier survival analysis with log-rank test in different subgroups. Multivariate survival analyses were performed using Cox regression model. Correlation analyses were performed to assess the possible linear relationship using Spearman correlation (ϱ), with a p-value < 0.05 considered significant. It is used mainly in our study to determine the link between the quantitative DWI (nADC) values and time to event (i.e., to death in days). A Spearman correlation factor of >0.4 was considered a strong relationship. All statistical analyses were performed using R (version 3.6.3; The R Foundation for Statistical Computing, Vienna, Austria) and SPSS statistical software (version 23.0 IBM Corp, Chicago, IL, US). A two-sided p-value < 0.05 was considered statistically significant.

Results

- 3.1 Demographic and treatment characteristics of sampled individuals.
- 3.2 Results of statistical correlation.
- 3.3 Results of Univariate Analysis; nADC in Relation to Molecular Markers.
- 3.4 Results of survival univariate analysis (i.e., Kaplan–Meier analysis):
    - 3.4.1 Defining nADC cutoff point as an independent variable (i.e., ROC curve analyses).
    - 3.4.2 Defining age cutoff point as an independent variable (i.e., ROC curve analyses).
    - 3.4.3 Effect of nADC on patients' survival using Kaplan–Meier survival analysis.
    - 3.4.4 Effect of age on patients' survival using Kaplan–Meier survival analysis.
- 3.5 Results of survival multivariate analysis (i.e., Cox regression analysis).

3.1 Demographic and Treatment Characteristics of Sampled Individuals

From January 2015 to January 2018, a total of 110 patients had a newly-diagnosed pathologically confirmed GBM in Health Sciences Center-Winnipeg, MB. Of these, 93 patients fulfilled the inclusion and exclusion criteria described in the methods. The basic demographics and type of surgery are shown in Table 1. **A total of 17 patients (15.5% of confirmed GBM cases) did not meet the inclusion criteria and were excluded for the following reasons:**

- Eleven patients did not have a preoperative MRI at the time of diagnosis
- Three patients had intratumoural hemorrhage, making calculation of the ADC value unreliable
- Two patients did not have DWI and ADC in the initial MRI.
- One patient had an infratentorial brainstem tumour

86 patients in our study reached the primary endpoint of the study (i.e., death) during the follow-up period constituting 92.5% of all patients included in the study.

		n	%
Age		59.79	
Gender	F	38	40.86
	M	55	59.14
Type of Surgery	GTR	9	9.68
	STR	71	76.34
	Biopsy	13	13.98

Table 1: Basic demographic profile and type of surgery of patients included in the study.

3.2 Results of Statistical Correlation

To study the correlation between nADC and time to death in days, Spearman's rho correlation was done as shown in Figure 1. A weak positive linear correlation was found (r=0.244 with a two-tailed p-value of 0.018). To study the correlation between age and nADC, Spearman's rho correlation was done as shown in Figure 2. A weak negative linear correlation was found (r=-0.223 with a two-tailed p-value of 0.031).

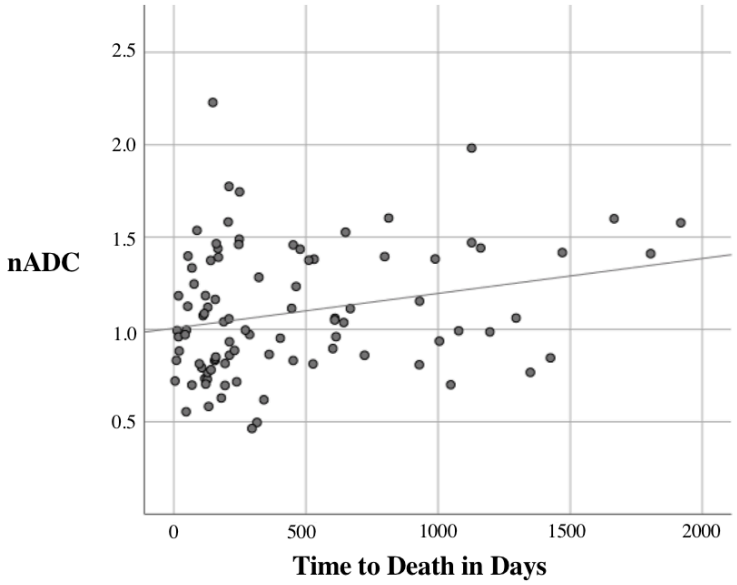

Figure 1: Scatter plot with fit line of the relationship between nADC (y-axis) and time to death in days (x-axis). nADC=Normalized Apparent Diffusion Coefficient.

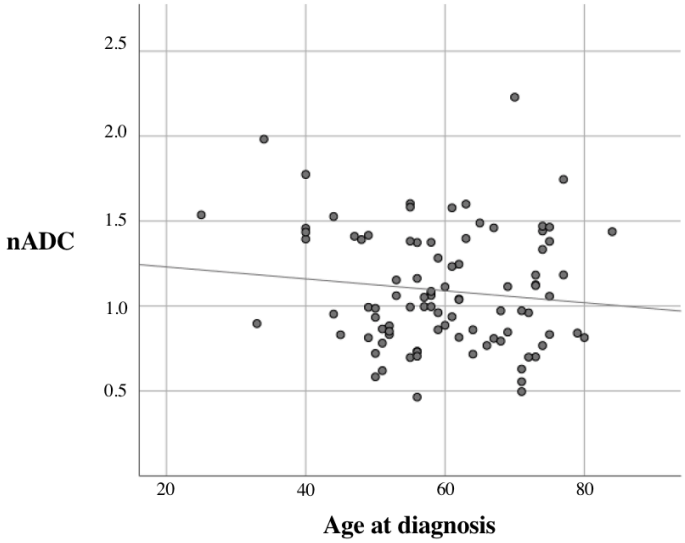

Figure 2: Scatter plot with fit line of the relationship between Age at diagnosis in years (x-axis) and time to death in days (y-axis). nADC=Normalized Apparent Diffusion Coefficient.

3.3 Results of Univariate Analysis; nADC in Relation to Molecular Markers

Table 2 shows nADC values in relation to molecular markers. The vast majority of patients in our cohort had IDH-wild tumors except five paitnets who had IDH-mutant tumors. IDH mutation status in relation to nADC was found to be significant (p-value of 0.015), as highlighted in red. The fact that IDH mutation status is available for all patients as part of the standard molecular and genetic testing of gliomas in our institution and as a standard of care in practice now makes this finding also clinically significant, in comparison to other molecular markers. All other molecular markers, including ATRX, MGMT, 1p/19q codeletion, and Ki67 (as a histopathological proliferation index), were found to be statistically insignificant.

		Mean nADC	SD	Mean diff	SE diff	P-value
IDH	wild	1.07	0.33	0.38	0.15	0.015*
	mutant	1.45	0.37			
TP53	wild	1.12	1.05	0.12	0.07	0.084
	mutant	1.05	0.39			
MGMT	unmethylated	1.13	0.41	0.03	0.12	0.811
	methylated	1.10	0.33			
1p/19q codeletion	Yes	0.99	0.19	0.09	0.15	0.522
	No	1.08	0.28			
Ki-67	<10	1.14	0.34	0.07	0.08	0.348
	>10	1.07	0.31			

Table 2: The t-test of mean differences of nADC for each molecular markers included in the study. "SD"= standard deviation. "SE"= standard error. "diff"= difference "*" indicates statistical significance.

3.4 Results of Survival Univariate Analysis (i.e., Kaplan–Meier Analysis)

To study the correlation between the different independent variables and survival, Kaplan–Meier analysis was used. This helped identifying which independent variables to include in the Cox multivariate regression model to be linked to survival. Variables with a p-value of <0.05 will be further assessed using the Cox regression. One of the issues and limitations of Kaplan–Meier analysis is defining clusters using categorical variables. This necessitates dichotomizing continuous variables of interest to be used in the multivariate Cox regression analysis model. In our case, the two continuous variables are age and nADC. Besides the need to dichotomize the mentioned continuous variables to perform the Kaplan–Meier analysis, there is a practical advantage in helping to interpret results and using data as a clinical tool. However, the cost might include losing information.

3.4.1 Defining nADC Cutoff Point as an Independent Variable (i.e., ROC Curve Analyses)

To define the cutoff point of nADC in relation to survival, a time-dependent ROC curve was used. The ROC curve for nADC as a continuous variable and survival in days shows a significant p-value of the area under the curve (AUC) of 0.015. When choosing a cutoff point of 1.1725, the sensitivity is 46% and specificity is 71%. The p-value of Cox regression multivariate analysis predicted by time-dependent ROC curves was 0.039 which is statistically significant. In a previous report, a cutoff point of 0.75 for nADC had a predictive survival value in the context of patients with GBM (Shankar et al., 2016). In our data, a cutoff point of 0.75 for nADC has a sensitivity of 97% and specificity of 23%. However, the p-value of Cox regression multivariate analysis predicted by time-dependent ROC curves becomes 0.19, which is not statistically significant.

3.4.2 Defining Age Cutoff Point as an Independent Variable (i.e., ROC Curve Analyses)

To define the cutoff point of age in relation to survival, time-dependent ROC curve was used. The ROC curve for age as a continuous variable and survival in days shows a significant p-value of AUC 0.003. When choosing a cutoff point of 70, the results were sensitivity of 54.3% and specificity of 37.9%. The p-value of Cox regression multivariate analysis predicted by time-dependent ROC curves was 0.016, which is statistically significant. That said, the age cutoff point to define the elderly population linked to worse outcomes in gliomas in the literature, and the one used to indicate the need to do MGMT methylation profile of tumours in our institution, is 55. In our data, a cutoff point of 55 results in a sensitivity of 54.3% and specificity of 37.9%. The p-value of Cox regression multivariate analysis predicted by time-dependent ROC curves becomes 0.29, which is not statistically significant.

3.4.3 Effect of nADC on Patients' Survival Using Kaplan–Meier Survival Analysis

To study the effect of nADC on survival, Kaplan–Meier Survival Analysis was used. As shown in Figure 3, the two-tailed p-value of log-rank (Mantel–Cox) is 0.046, which is statistically significant when using a cutoff point of 1.1725 for nADC to stratify patients with GBM. The median survival is 11.5 months for nADC > 1.1725 vs. 7.5 months for nADC < 1.1725. When using a cutoff point of 0.75 for nADC, which is not supported by our time-dependent ROC curves in the context of our data but proposed by a previous study (Jai Jai Shiva, Adil, & Namita, 2018), the two-tailed p-value log-ranking (Mantel–Cox) is 0.017, which is statistically significant (Figure 4). Median survival is 15 months for nADC >0.75 vs 9.5 months for nADC <0.75, which is also clinically meaningful too.

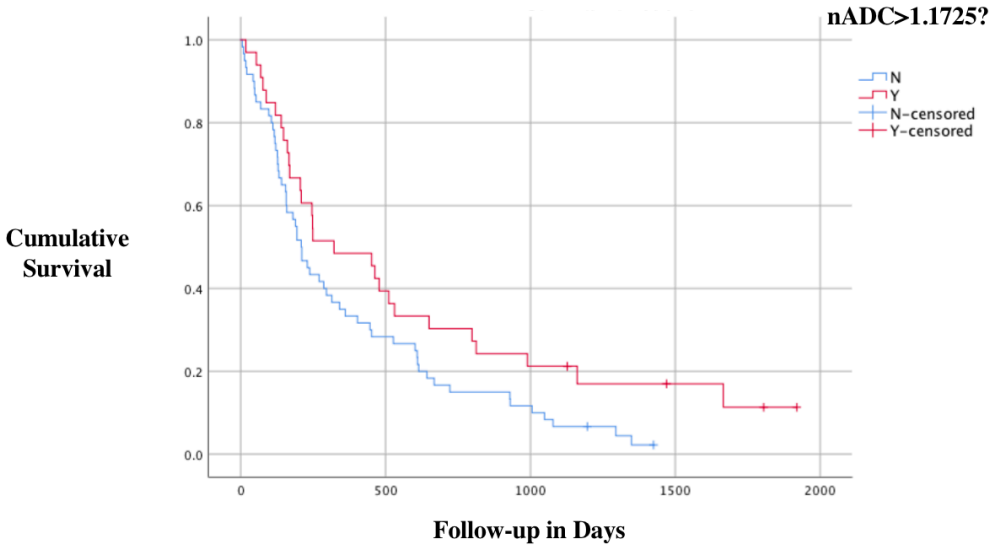

Figure 3: Kaplan-Meier survival function curves, grouped by nADC cut off of 1.1725. The two-tailed p-value of Log rank (Mantel-Cox) is 0.046 which is statistically significant. The median survival is 11.5 months for nADC>1.1725 vs 7.5 months for nADC<1.1725. nADC=Normalized Apparent Diffusion Coefficient. nADC=Normalized Apparent Diffusion Coefficient.

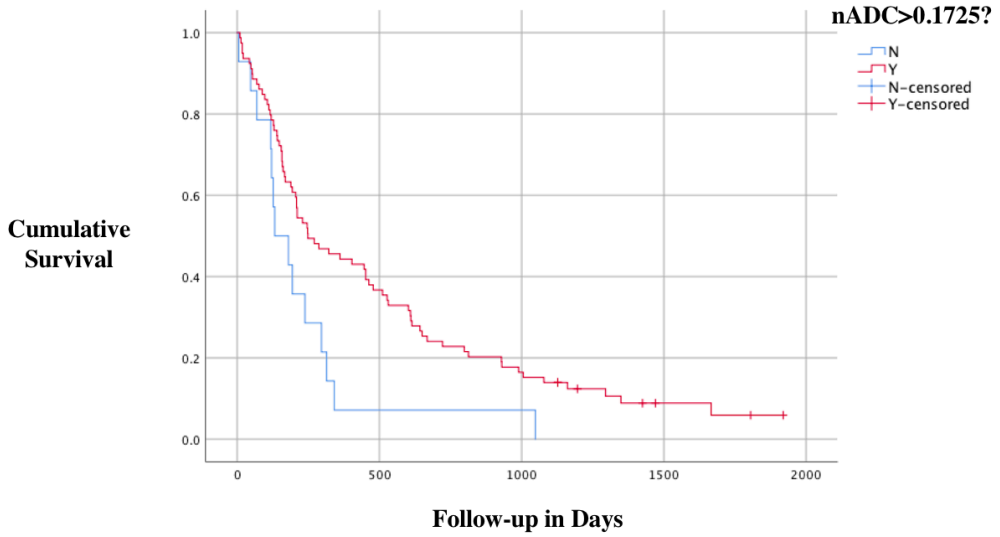

Figure 4: Kaplan-Meier survival function curves, grouped by nADC cut off of 0.75. The two-tailed p-value of Log rank (Mantel-Cox) is 0.017 which is statistically significant. Median survival is 15 months for nADC>0.75 vs 9.5 months for nADC<0.75. nADC=Normalized Apparent Diffusion Coefficient.

3.4.4 Effect of Age on Patients' Survival Using Kaplan–Meier Survival Analysis

To study the effect of age on survival, Kaplan–Meier Survival Analysis was used. As shown in Figure 5, the two-tailed p-value of log-rank (Mantel–Cox) is 0.02, which is statistically significant when using a cutoff point of 70 for age.. The median survival is 10.6 months for Age <70 vs. 5.6 months for Age >70. When using a cutoff point of 55 for age (which is proposed by literature as a definition of the elderly population linked to worse outcome in gliomas), the two-tailed p-value of log-rank (Mantel–Cox) is 0.043, which is statistically significant (Figure 4). Median survival is 16.14 months for Age <55 vs. 6.9 months for Age >55.

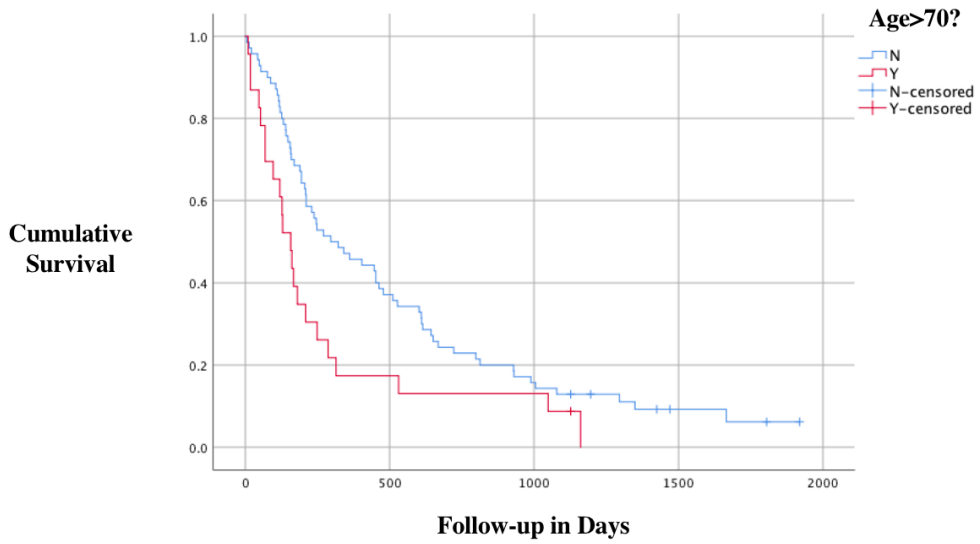

Figure 5: Kaplan-Meier survival function curves, grouped by age cut off of 70. The two-tailed p-value of Log rank (Mantel-Cox) is 0.02 which is statistically significant when using a cut-off point of 70 for age. The median survival is 10.6 months for Age<70 vs 5.6 months for Age>70.

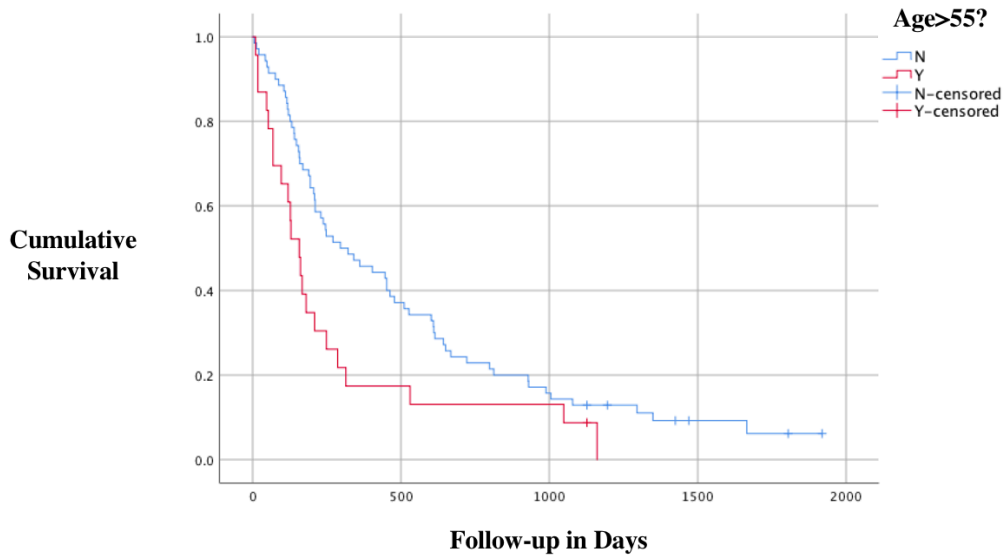

Figure 6: Kaplan-Meier survival function curves, grouped by age cut off of 55. The the two-tailed p-value of Log rank (Mantel-Cox) is 0.043 which is statistically significant. Median survival is 16.14 months for Age<55 vs 6.9 months for Age>55.

3.5 Results of Survival Multivariate Analysis (i.e., Cox Regression Analysis)

To study the impact of the different independent variables linked to survival of GBM patients, multivariate Cox regression analysis was used to adjust for possible confounders. Compared to univariate analysis, this will control and adjust for all the independent variables in our model, including nADC, age, IDH mutation status, and type of surgery, as shown in Table 3. We found that age (p-value of 0.016) and nADC (p-value of 0.039) are statistically significant. Furthermore, Cox regression analysis showed that age was negatively and nADC positively correlated to the OS of patients.

Regarding nADC in our cohort, individuals with nADC <1.1725 had a mortality hazard that was 1.69 times that of individuals with nADC >1.1725 after adjusting for covariates of age, IDH mutation status, and type of surgery. In other words, individuals with nADC <1.1725 were associated with an increased mortality hazard of 69% compared to individuals with nADC >1.1725 after adjusting for covariates of age, IDH mutation status, and type of surgery.

Regarding age in our cohort, individuals <70-year-old had a mortality hazard that was 0.53 times that of individuals >70-year-old old after adjusting for covariates of nADC, IDH mutation status, and type of surgery. In other words, individuals < 70-year-old had a reduced mortality hazard of 47% compared to individuals > 70-year-old old after adjusting for covariates of nADC, IDH mutation status, and type of surgery.

		p-value	HR	95% CI
nADC	>1.1725	*Reference*		
	<1.1725	0.032*	1.69	1.05-2.8
Age	>70	*Reference*		
	<70	0.016*	0.53	0.31-0.89
IDH	mutant	*Reference*		
	wild	0.479	1.53	0.47-5.04
Type of Surgery	GTR	*Reference*		
	STR	0.876	0.93	0.37-2.31
	Biopsy	0.624	1.17	0.63-2.18

Table 3: Results for Cox proportional hazards model of survival adjusting for nADC, age, IDH mutation status, and type of surgery covariates. nADC=Normalized Apparent Diffusion Coefficient. HR= hazard ratio. CI= confidence interval. "*" indicates statistical significance.

4. Discussion

- 4.1 The Real Challenge with GBM.
- 4.2 Diffusion MRI Metrics as Possible Novel Noninvasive Biomarkers.
- 4.3 Linking Diffusion MRI to Molecular Profile of GBML The Novelty of This Study.
- 4.4 The Nature of Isolated Restricted Diffusion Foci in GBM.
- 4.5 Diffusion Imaging Metrics: nADC vs. Mean ADC.
- 4.6 The Role of Diffusion Imaging in the Management of GBM.
- 4.7 The Role of Diffusion Imaging in the Recurrence of GBM.
- 4.8 Limitations.
- 4.9 Future directions.

4.1 The Real Challenge with GBM

The identification of various genomic and molecular features in gliomas has enhanced our understanding and treatment of these patients (Herbert et al., 2011). In particular, markers such as IDH mutation and MGMT methylation status have enhanced our ability to predict individual patient treatment responses and present future opportunities for individually targeted treatment (Brat et al., 2020) However, despite this, progress the survival of patients with GBMs is highly variable making individual management challenging. Here we have identified that patients with an nADC <1.1725 had an increased mortality hazard of 69% compared to individuals with nADC >1.1725 after adjusting for covariates of age, gender, and IDH mutation status. This demonstrates that nADC along with other factors might better predict survival.

4.2 Diffusion MRI Metrics as Possible New Noninvasive Biomarkers

Multiple diffusion MRI metrics have been linked to cellularity, necrosis, and hemorrhage at a histopathological level, justifying the growing interest in their application in brain tumours (Kono et al., 2001). For example, lower ADC map values have been linked to hypercellularity, whereas higher values have been linked to edema and necrosis (Kono et al., 2001). Diffusion MRI has many advantages as a unique imaging modality because it is widely available. This is in comparison to perfusion MRI, which has limited access related to hardware and software availability. Diffusion MRI is quick and does not require the injection of contrast. It is also more reproducible, and because of its quantitative nature, the intra- and interobserver variability is considered to be within the acceptable range (Kono et al., 2001)

4.3 Linking Diffusion MRI to the Molecular Profile of GBM: The Novelty of This Study

A previously reported study investigated the link between nADC and survival in GBM patients (Shankar et al., 2016). However, in this study only histopathological data were used. By adding the tumors molecular features into the analysis allows a more comprehensive understanding of the relationship between nADC and survival. Although the link between nADC and survival was established in both studies, we reproduced these findings with Spearman's rho correlation of 0.244, indicating a positive but weak linear correlation. This is in comparison to the previous study reporting a stronger relationship of 0.39 which is considered a moderate to strong relationship (Shankar et al., 2016).

We found that nADC was lower in IDH-wild GBM versus IDH-mutant astrocytoma with a p-value of 0.015. Our study showed that the two-tailed p-value of log-rank (Mantel–Cox) is statistically significant (0.046) when using a cutoff point of 1.1725 for nADC to stratify patients with GBM. The median survival is 11.5 months for nADC > 1.1725 vs. 7.5 months for nADC<1.1725. When linking that to the molecular profile of tumours in our data, 4 out of 5 patients (80%) with IDH-mutant astrocytoma have nADC above the proposed cutoff point of 1.1725 which might contribute to the explanation of a better survival profile. However, this is a small portion of patients with nADC >1.1725 (only 12.12%); necessitates the use of Cox regression analysis to understand the complexity of interaction with other factors such as age and extent of resection along with IDH mutation status. Age showed a two-tailed p-value log-rank (Mantel–Cox) of 0 0.02, which is statistically significant when using a cutoff point of 70 for age. The median survival 10.6 months for Age<70 v.s 5.6 months for age >70.

Considering the multiple interacting and confounding factors, nADC and age stand out as variables independently predicting survival. Adjusting for age, IDH mutation status, and extent of resection, nADC conferred a survival-predicting advantage by showing that nADC <1.1725 had a mortality hazard that was 1.69 times that of individuals with nADC >1.1725. Because this multivariate survival advantage takes into account IDH mutation status, nADC brings meaningful insight about survival that goes beyond its simple association with IDH mutation status.

As mentioned in the results section, the age cutoff point to define the elderly population linked to worse outcomes in gliomas in the literature is 55. It is also the age cutoff point for requesting genetic sequencing for GBM in our institution since the vast majority of patients with age >55 have IDH-wild tumors (c-impact 5 (Brat et al., 2020)). However, choosing a cutoff point of 70 had a survival advantage in the multivariate Cox regression analysis predicted by time-dependent ROC curves in our data. It is interesting to mention that after adjusting for IDH mutation status, a cutoff point of age of 55 was not found to be significant. This might indicate that the age cutoff of 55 might be a reflection of IDH mutation status indirectly. By contrast, a cutoff point of age of 70 was found to be an independent variable predicting poor outcome, as shown in the Cox regression analysis model.

4.4 The Nature of Isolated Restricted Diffusion Foci in GBM

In the literature, the contrast enhancing areas in GBM gained much attention historically. More recently, foci of restricted diffusion in GBMs have been linked to survival in GBM patients as well. Establishing the relationship between the degree of restriction of these foci representing the lowest nADC values can suggest the potential degree of malignancy it carries. Because studying the pattern of enhancement and its correlation with restricted diffusion is outside the scope of this study, more research is needed to investigate its potential role.

4.5 Diffusion Imaging Metrics: nADC vs. Mean ADC

Multiple diffusion MRI metrics can be used to quantify a tumor's degree of restricted diffusion. Although our study used nADC which has the advantage of comparing the lowest possible ADC value of the tumour to the contralateral normal white matter side as a reference, other studies have investigated the role of minimal ADC value and mean ADC. They both have been reported to be associated with predicting poor survival in patients with GBM; however, the minimal ADC might be superior to mean ADC because it might represent the most malignant part of the tumour. The issue with mean ADC values is that GBMs are mostly heterogeneous tumours in nature, meaning maximal ADC values, in comparison to minimal ADC values, get diluted in the less malignant part of the tumour (including possible edema) and thus might not reflect the true degree of malignancy. The volume of the ADC was not included in the study because of the lack of volumetric analysis tools in the imaging software and the fact that it wasn't found to be statistically significant in relation to survival (Shankar et al., 2016).

4.6 The Role of Diffusion Imaging in the Management of GBM

Our findings suggest that diffusion MRI metrics at the time of initial diagnosis can serve as a component in a composite predictive biomarker that includes other independent variables to define patients with better survival profiles. Previous studies have reported that nADC was used to determine the appropriate extent of resection for patients with GBM. In one study, GBM patients with an nADC with a value <0.75 at the time of diagnosis improved their survival only when gross total resection was achieved in comparison to subtotal resection or biopsy (Shankar et al., 2016). This is in comparison to GBM patients with nADC >0.75 who had a survival advantage with either partial or gross total resection. However, this finding was not reproduced in our study.

4.7 The Role of Diffusion Imaging in the Recurrence of GBM

Diffusion MRI is part of standard MRI protocol for GBM patients with possible tumour recurrence or progression. Although this is outside the scope of our study, our findings establish a link between the nADC values and survival (possibly through molecular signature). This entertains the idea of a role in the diagnosis of GBM recurrence and confirms some reports based on histopathological examination—mostly that isolated foci of restricted diffusion can aid in the diagnosis of progression and in the context of pseudoprogression (Clarke, Schmidt, & Pickett, 2017). However, further prospective large studies are needed to establish the role of nADC values in the context of tumor recurrence.

4.8 Limitations

The first and primary limitation of this study is related to its retrospective design. Compared to prospective studies, retrospective studies have many disadvantages. Specifically, in the context of our study, major key statistical tools cannot be measured. In addition, a long list of biases can affect the selection of participants in the study. Especially with the small sample size we included, retrospective studies make it more difficult to assess the relationship to rare outcomes (Bulakbasi et al., 2004). Nevertheless, the follow-up period for the cohort of patients with GBM was adequate to ensure a good proportion of patients reached the event (death) related to the primary endpoint of interest within this period. In our cohort, 92.5% of all patients included in the study reached the primary endpoint.

The second limitation of the study is the small number of patients included. The need to exclude 15.5% of confirmed GBM cases further compromised the total number. Within the study's period of interest, patients were excluded because of the lack of preoperative MRI at the time of diagnosis. They also were excluded because of the lack of diffusion maps of DWI and ADC in the MRI at the time of diagnosis and the presence of intratumoural hemorrhages, which makes calculating ADC values unreliable. This also affects finding a reasonable number of patients with IDH-mutant astrocytoma to be able to shed light on the role of nADC in recognizing the IDH mutation status.

Third, our study used only OS as the primary endpoint of interest without the commonly used variable PFS. The rationale was related to the uniqueness of GBM as a disease entity with an extremely short survival time, making OS as a time-to-death statistical tool more feasible and definitive. In addition, PFS might enable quicker completion of a study instead of waiting to reach death as an event in general. However, PFS does not always

translate into OS and is subject to biases. Moreover, there can be many different definitions of PFS across different studies attempting to answer the same question. In brain tumours in particular, some studies define PFS based on imaging variables, whereas others use clinical manifestations. In addition, it is more difficult to establish a meaningful clinical benefit from PFS compared to OS as an endpoint.

Fourth, we did not analyze the role of adjuvant treatment (e.g., radiation therapy and chemotherapy) and its impact on survival. To gain access to data related to treatment details, we attempted to align this project with a study on that topic being done in the same institution. Unfortunately, there was some delay in the process of acquiring approval that was beyond the author's control. However, the vast majority of GBM patients in our institution are given similar adjuvant therapy following a standard treatment protocol. Thus it is likely that the basic analyses presented here would yield similar results.

Fifth, although some papers have found a correlation between diffusion MRI metrics and histopathological features (e.g., necrosis, edema, and microvascular proliferation) (Rose et al., 2013), the focus of our study was to find the association between diffusion MRI metrics and molecular/genetic features. For that reason, and except for Ki67 as a proliferation index, no histopathological features were correlated to diffusion MRI metrics in this study.

Sixth, quantitative values in imaging have the advantage of decreasing observer variability based on categorical morphological features. Nevertheless, there is room for different values among observers (i.e., issues of reproducibility and reliability) when defining the area with the lowest ADC value in the tumour and when defining NAWM. Because the

recording of imaging data is based on a single individual, analysis of interobserver variability was not possible.

Seventh, our local data focused on the basic protocol of brain tumour molecular analysis. Further molecular analysis might address questions beyond the scope of this study. An example would be epidermal growth factor receptor (EGFR) expression, which is not assessed consistently for our local patients.

Last, continuous variables were commonly analyzed as dichotomous/categorical variables according to the institutional reference ranges or correlations from the ROC curves. Dichotomous variables are used broadly to gain a practical advantage of the results as a clinical tool, simplify the statistical analysis, and help present and interpret the data. However, there are costs for dichotomizing data, including losing information, decreasing statistical power, and underestimating the extent of variation in outcome between groups.

4.9 Future Directions

From a purely technical point of view, the most disappointing aspect of diffusion MRIs is their lack of standardization (Langen, Galldiks, Hattingen, & Shah, 2017; Nie, Zhang, Adeli, Liu, & Shen, 2016; Pujol et al., 2015). Nevertheless, there is a continued effort to standardize diffusion MRI acquisition variables and their analytical methods. Automation has been suggested as the most effective way to standardize diffusion MRIs across different institutions and protocols. For that reason, there is a growing interest in applying the different techniques of artificial intelligence to the world of medical imaging. These methods, including machine learning and deep learning tools, can be used to better understand the

complexity of the association between diffusion MRI metrics and survival in GBM patients (Chang et al., 2015; Nie et al., 2016; Petrova et al., 2019).

5.0 Conclsion

nADC might have some value in identifying GBM patients with worse survival via IDH-mutation status.

5. References

Aum, D. J., Kim, D. H., Beaumont, T. L., Leuthardt, E. C., Dunn, G. P., & Kim, A. H. (2014). Molecular and cellular heterogeneity: The hallmark of glioblastoma. *Neurosurgical Focus, 37*(6). doi:10.3171/2014.9.FOCUS14521

Babsky, A. M., Hekmatyar, S. K., Zhang, H., Solomon, J. L., & Bansal, N. (2006). Predicting and monitoring response to chemotherapy by 1,3-bis(2- chloroethyl)-1-nitrosourea in subcutaneously implanted 9L glioma using the apparent diffusion coefficient of water and 23Na MRI. *Journal of Magnetic Resonance Imaging, 24*(1), 132-139. doi:10.1002/jmri.20615

Bailey, P., & Cushing, H. (1926). *A classification of the tumors of the glioma group on a histogenetic basis with a correlated study of prognosis*: Lippincott.

Brat, D. J., Aldape, K., Colman, H., Figrarella-Branger, D., Fuller, G. N., Giannini, C., . . . Komori, T. (2020). cIMPACT-NOW update 5: recommended grading criteria and terminologies for IDH-mutant astrocytomas. *Acta neuropathologica, 139*(3), 603-608.

Bulakbasi, N., Guvenc, I., Onguru, O., Erdogan, E., Tayfun, C., & Ucoz, T. (2004). The added value of the apparent diffusion coefficient calculation to magnetic resonance imaging in the differentiation and grading of malignant brain tumors. *Journal of Computer Assisted Tomography, 28*(6), 735-746. doi:10.1097/00004728-200411000-00003

Bulakbasi, N., Kocaoglu, M., Örs, F., Tayfun, C., & Ügöz, T. (2003). Combination of single-voxel proton MR spectroscopy and apparent diffusion coefficient calculation in the evaluation of common brain tumors. *American Journal of Neuroradiology, 24*(2), 225-233.

Chakhoyan, A., Woodworth, D. C., Harris, R. J., Lai, A., Nghiemphu, P. L., Liau, L. M., . . . Ellingson, B. M. (2018). Mono-exponential, diffusion kurtosis and stretched exponential diffusion MR imaging response to chemoradiation in newly diagnosed glioblastoma. *Journal of Neuro-Oncology, 139*(3), 651-659. doi:10.1007/s11060-018-2910-9

Chang, W., Pope, W. B., Harris, R. J., Hardy, A. J., Leu, K., Mody, R. R., . . . Ellingson, B. M. (2015). Diffusion MR characteristics following concurrent radiochemotherapy predicts progression-free and overall survival in newly diagnosed glioblastoma. *Tomography, 1*, 37-43.

Chen, J., Xia, J., Zhou, Y. C., Xia, L. M., Zhu, W. Z., Zou, M. L., . . . Wang, C. Y. (2005). Correlation between magnetic resonance diffusion weighted imaging and cell density in astrocytoma. *Zhonghua zhong liu za zhi [Chinese journal of oncology], 27*(5), 309-311.

Chenevert, T. L., Sundgren, P. C., & Ross, B. D. (2006). Diffusion Imaging: Insight to Cell Status and Cytoarchitecture. *Neuroimaging Clinics of North America, 16*(4), 619-632. doi:10.1016/j.nic.2006.06.005

Clarke, B., Schmidt, M., & Pickett, G. (2017). P. 043 Presence of infiltrative glioblastoma cells in an isolated area of diffusion restriction. *Canadian Journal of Neurological Sciences, 44*(S2), S24-S25.

Çoban, X. G., Mohan, S., Kural, F., Wang, S., O'Rourke, D. M., & Poptani, H. (2015). Prognostic value of dynamic susceptibility contrast-enhanced and diffusion-weighted mr imaging in patients with glioblastomas. *American Journal of Neuroradiology, 36*(7), 1247-1252. doi:10.3174/ajnr.A4284

Davis, M. E. (2016). Glioblastoma: Overview of disease and treatment. *Clinical Journal of Oncology Nursing, 20*(5), 1-8. doi:10.1188/16.CJON.S1.2-8

Deike, K., Wiestler, B., Graf, M., Reimer, C., Floca, R. O., Bäumer, P., . . . Radbruch, A. (2016). Prognostic value of combined visualization of MR diffusion and perfusion maps in glioblastoma. *Journal of Neuro-Oncology, 126*(3), 463-472. doi:10.1007/s11060-015-1982-z

Drake-Pérez, M., Boto, J., Fitsiori, A., Lovblad, K., & Vargas, M. I. (2018). Clinical applications of diffusion weighted imaging in neuroradiology. *Insights into Imaging, 9*(4), 535-547. doi:10.1007/s13244-018-0624-3

Friedmann-Morvinski, D. (2014). Glioblastoma heterogeneity and cancer cell plasticity. *Critical Reviews in Oncogenesis, 19*(5), 327-336. doi:10.1615/CritRevOncog.2014011777

Gauvain, K. M., McKinstry, R. C., Mukherjee, P., Perry, A., Neil, J. J., Kaufman, B. A., & Hayashi, R. J. (2001). Evaluating pediatric brain tumor cellularity with diffusion-tensor imaging. *American Journal of Roentgenology, 177*(2), 449-454. doi:10.2214/ajr.177.2.1770449

Gupta, A., Young, R., Karimi, S., Sood, S., Zhang, Z., Mo, Q., . . . Lassman, A. (2011). Isolated diffusion restriction precedes the development of enhancing tumor in a subset of patients with glioblastoma. *American Journal of Neuroradiology, 32*(7), 1301-1306.

Herbert, C., Williams, M., Sawyer, H., Greenslade, M., Cornes, P., & Hopkins, K. (2011). Treatment of Glioblastoma Multiforme with Radiotherapy and Concomitant and Adjuvant Temozolomide: Translation of Randomised Controlled Trial Evidence into Routine Clinical Practice. *Clinical Oncology, 23*(5), 372-373. doi:10.1016/j.clon.2011.01.157

Jai Jai Shiva, S., Adil, B., & Namita, S. (2018). Isolated Diffusion Restriction Preceding Contrast Enhancement in Glioblastoma Multiforme is Associated with Short-Term Survival. *OBM Neurobiology, 2*(4), 1-1.

Khan, U. A., Rennert, R. C., White, N. S., Bartsch, H., Farid, N., Dale, A. M., & Chen, C. C. (2018). Diagnostic utility of restriction spectrum imaging (RSI) in glioblastoma patients after concurrent radiation-temozolomide treatment: A pilot study. *Journal of Clinical Neuroscience, 58*, 136-141. doi:10.1016/j.jocn.2018.09.008

Kleihues, P., & Cavenee, W. (2000). WHO classification of tumours. *Pathology & genetics. Tumors of the nervous system. Lyon, France: IARCpress.*

Kono, K., Inoue, Y., Nakayama, K., Shakudo, M., Morino, M., Ohata, K., . . . Yamada, R. (2001). The role of diffusion-weighted imaging in patients with brain tumors. *Ajnr: American Journal of Neuroradiology, 22*(6), 1081-1088. Retrieved from http://proxycheck.lib.umanitoba.ca/libraries/online/proxy.php?http://ovidsp.ovid.com/ovidweb.cgi?T=JS&CSC=Y&NEWS=N&PAGE=fulltext&D=med4&AN=11415902
https://search.lib.umanitoba.ca/openurl/01UMB_INST/01UMB_INST:UMB?sid=OVID:medline&id=pmid:11415902&id=doi:&issn=0195-6108&isbn=&volume=22&issue=6&spage=1081&pages=1081-8&date=2001&title=Ajnr%3A+American+Journal+of+Neuroradiology&atitle=The+role+of+diffusion-weighted+imaging+in+patients+with+brain+tumors.&aulast=Kono&pid=%3Cauthor%3EKono+K%2CInoue+Y%2CNakayama+K%2CShakudo+M%2CMorino+M%2COhata+K%2CWakasa+K%2CYamada+R%3C%2Fauthor%3E%3CAN%3E11415902%3C%2FAN%3E%3CDT%3EJournal+Article%3C%2FDT%3E

Krishnan, A. P., Karunamuni, R., Leyden, K. M., Seibert, T. M., Delfanti, R. L., Kuperman, J. M., . . . White, N. S. (2017). Restriction spectrum imaging improves risk stratification in patients with glioblastoma. *American Journal of Neuroradiology, 38*(5), 882-889. doi:10.3174/ajnr.A5099

Langen, K.-J., Galldiks, N., Hattingen, E., & Shah, N. J. (2017). Advances in neuro-oncology imaging. *Nature Reviews Neurology, 13*(5), 279-289.

Louis, D. N., Perry, A., Reifenberger, G., Von Deimling, A., Figarella-Branger, D., Cavenee, W. K., . . . Ellison, D. W. (2016). The 2016 World Health Organization classification of tumors of the central nervous system: a summary. *Acta neuropathologica, 131*(6), 803-820.

Macdonald, D. R., Cascino, T. L., Schold Jr, S. C., & Cairncross, J. G. (1990). Response criteria for phase II studies of supratentorial malignant glioma. *Journal of Clinical Oncology, 8*(7), 1277-1280.

Madsen, H., Hellwinkel, J. E., & Graner, M. W. (2015). Clinical trials in glioblastoma — designs and challenges. *Molecular considerations and evolving surgical management issues in the treatment of patients with a brain tumor*.

Mallick, S., Benson, R., Hakim, A., & Rath, G. K. (2016). Management of glioblastoma after recurrence: A changing paradigm. *Journal of the Egyptian National Cancer Institute, 28*(4), 199-210.

Neal, M. L., Trister, A. D., Cloke, T., Sodt, R., Ahn, S., Baldock, A. L., . . . Swanson, K. R. (2013). Discriminating Survival Outcomes in Patients with Glioblastoma Using a Simulation-Based, Patient-Specific Response Metric. *PLoS ONE, 8*(1). doi:10.1371/journal.pone.0051951

Nie, D., Zhang, H., Adeli, E., Liu, L., & Shen, D. (2016). *3D deep learning for multi-modal imaging-guided survival time prediction of brain tumor patients*. Paper presented at the International conference on medical image computing and computer-assisted intervention.

Nuzzo, S., Brancato, V., Affinito, A., Salvatore, M., Cavaliere, C., & Condorelli, G. (2020). The role of RNA and dna aptamers in glioblastoma diagnosis and therapy: a systematic review of the literature. *Cancers, 12*(8), 2173.

Ohgaki, H., & Kleihues, P. (2013). The definition of primary and secondary glioblastoma. *Clinical Cancer Research, 19*(4), 764-772.

Parsons, D. W., Jones, S., Zhang, X., Lin, J. C., Leary, R. J., Angenendt, P., . . . Kinzler, K. W. (2008). An integrated genomic analysis of human glioblastoma multiforme. *Science, 321*(5897), 1807-1812. doi:10.1126/science.1164382

Petrova, L., Korfiatis, P., Petr, O., LaChance, D. H., Parney, I., Buckner, J. C., & Erickson, B. J. (2019). Cerebral blood volume and apparent diffusion coefficient – Valuable predictors of non-response to bevacizumab treatment in patients with recurrent glioblastoma. *Journal of the Neurological Sciences, 405*. doi:10.1016/j.jns.2019.116433

Pope, W. B., Prins, R. M., Albert Thomas, M., Nagarajan, R., Yen, K. E., Bittinger, M. A., . . . Liau, L. M. (2012). Non-invasive detection of 2-hydroxyglutarate and other metabolites in IDH1 mutant glioma patients using magnetic resonance spectroscopy. *J Neurooncol, 107*(1), 197-205. doi:10.1007/s11060-011-0737-8

Pope, W. B., Qiao, X. J., Kim, H. J., Lai, A., Nghiemphu, P., Xue, X., . . . Cloughesy, T. (2012). Apparent diffusion coefficient histogram analysis stratifies progression-free and overall survival in patients with recurrent GBM treated with bevacizumab: A multi-center study. *Journal of Neuro-Oncology, 108*(3), 491-498. doi:10.1007/s11060-012-0847-y

Pujol, S., Wells, W., Pierpaoli, C., Brun, C., Gee, J., Cheng, G., . . . Stamm, A. (2015). The DTI challenge: toward standardized evaluation of diffusion tensor imaging tractography for neurosurgery. *Journal of Neuroimaging, 25*(6), 875-882.

Rose, S., Fay, M., Thomas, P., Bourgeat, P., Dowson, N., Salvado, O., . . . Crozier, S. (2013). Correlation of MRI-derived apparent diffusion coefficients in newly diagnosed

gliomas with [18F]-Fluoro-L-Dopa PET: What are we really measuring with minimum ADC? *American Journal of Neuroradiology, 34*(4), 758-764. doi:10.3174/ajnr.A3315

Rossignol, J., Srinageshwar, B., & Dunbar, G. L. (2020). Current therapeutic strategies for glioblastoma. *Brain Sciences, 10*(1). doi:10.3390/brainsci10010015

Saksena, S., Jain, R., Narang, J., Scarpace, L., Schultz, L. R., Lehman, N. L., . . . Mikkelsen, T. (2010). Predicting survival in glioblastomas using diffusion tensor imaging metrics. *Journal of magnetic resonance imaging : JMRI, 32*(4), 788-795. doi:10.1002/jmri.22304

Salcman, M. (2001). Glioblastoma multiforme and anaplastic astrocytoma. *Brain Tumors: An Encyclopedic Approach*, 493-523.

Schmainda, K. M. (2012). Diffusion-weighted MRI as a biomarker for treatment response in glioma. *CNS oncology, 1*(2), 169-180. doi:10.2217/cns.12.25

Seystahl, K., Hentschel, B., Loew, S., Gramatzki, D., Felsberg, J., Herrlinger, U., . . . the German Glioma, N. (2020). Bevacizumab versus alkylating chemotherapy in recurrent glioblastoma. *Journal of Cancer Research and Clinical Oncology, 146*(3), 659-670. doi:10.1007/s00432-019-03086-9

Shankar, J. J. S., Bata, A., Ritchie, K., Hebb, A., & Walling, S. (2016). Normalized apparent diffusion coefficient in the prognostication of patients with glioblastoma multiforme. *Canadian Journal of Neurological Sciences, 43*(1), 127-133.

Shukla, G., Alexander, G. S., Bakas, S., Nikam, R., Talekar, K., Palmer, J. D., & Shi, W. (2017). Advanced magnetic resonance imaging in glioblastoma: A review. *Chinese Clinical Oncology, 6*(4). doi:10.21037/cco.2017.06.28

Stupp, R., Mason, W. P., Van Den Bent, M. J., Weller, M., Fisher, B., Taphoorn, M. J. B., . . . Mirimanoff, R. O. (2005). Radiotherapy plus concomitant and adjuvant temozolomide for glioblastoma. *New England Journal of Medicine, 352*(10), 987-996. doi:10.1056/NEJMoa043330

Tomura, N., Narita, K., Izumi, J. I., Suzuki, A., Anbai, A., Otani, T., . . . Watarai, J. (2006). Diffusion changes in a tumor and peritumoral tissue after stereotactic irradiation for brain tumors: Possible prediction of treatment response. *Journal of Computer Assisted Tomography, 30*(3), 496-500. doi:10.1097/00004728-200605000-00024

van Dijken, B. R., van Laar, P. J., Smits, M., Dankbaar, J. W., Enting, R. H., & van der Hoorn, A. (2019). Perfusion MRI in treatment evaluation of glioblastomas: Clinical relevance of current and future techniques. *Journal of Magnetic Resonance Imaging, 49*(1), 11-22.

Yan, J. L., Van Der Hoorn, A., Larkin, T. J., Boonzaier, N. R., Matys, T., & Price, S. J. (2017). Extent of resection of peritumoral diffusion tensor imaging-detected abnormality as a predictor of survival in adult glioblastoma patients. *Journal of Neurosurgery, 126*(1), 234-241. doi:10.3171/2016.1.JNS152153

Zhang, P., & Liu, B. (2020). Differentiation among glioblastomas, primary cerebral lymphomas, and solitary brain metastases using diffusion-weighted imaging and diffusion tensor imaging: A PRISMA-compliant meta-analysis. *ACS Chemical Neuroscience, 11*(3), 477-483.

Zulch, K. J. (1979). Histological typing of tumours of the central nervous system. *International histological classification of tumours No 21.*, 19-24.